RAPID COMMUNICATIONS

PHYSICAL REVIEW D VOLUME 40, NUMBER 5 1 SEPTEMBER 1989

Search for $K_L^0 \to \mu e$ and $K_L^0 \to ee$ decays

T. Inagaki, M. Kobayashi, T. Sato, T. Shinkawa, F. Suekane, K. Takamatsu, and Y. Yoshimura
National Laboratory for High Energy Physics (KEK), Tsukuba, Ibaraki 305, Japan

K. Ishikawa, T. Kishida, T. K. Komatsubara, M. Kuze, F. Sai,* J. Toyoura,† and S. S. Yamamoto
Department of Physics, University of Tokyo, Bunkyo, Tokyo 113, Japan

Y. Hemmi
Department of Physics, Kyoto University, Sakyo, Kyoto 606, Japan
(Received 22 May 1989)

We report on the present status of a search for the rare decays $K_L^0 \to \mu e$ and $K_L^0 \to ee$ at the KEK 12-GeV Proton Synchrotron. We found no $K_L^0 \to \mu e$ or $K_L^0 \to ee$ events and found 54 $K_L^0 \to \mu\mu$ events. The upper limits of the $K_L^0 \to \mu e$ and $K_L^0 \to ee$ branching ratios are $B(K_L^0 \to \mu e) < 4.3 \times 10^{-10}$ and $B(K_L^0 \to ee) < 5.6 \times 10^{-10}$ at 90% confidence level. The 54 $K_L^0 \to \mu\mu$ events correspond to an absolute branching ratio of $(8.4 \pm 1.1) \times 10^{-9}$.

The $K_L^0 \to \mu e$ decay is a lepton-flavor-violating process which is forbidden by the standard model. Despite several experimental searches with increasing sensitivity this decay has not been found,[1,2] and the current upper limit on the branching ratio is $B(K_L^0 \to \mu e) < 1.9 \times 10^{-9}$.[2] The $K_L^0 \to ee$ decay is allowed by the standard model, but the branching ratio is predicted to be as small as 5×10^{-12},[3] and the experimental upper limit is $B(K_L^0 \to ee) < 1.2 \times 10^{-9}$.[4] Therefore, positive signals for these decays at the sensitivity of our experiment, which is about 10^{-11}, would imply the existence of a new physics.[5] The present report is based on about one half of the expected number of K_L^0's for the first round of this search.

K_L^0's are produced by a slow extracted proton beam from the KEK 12-GeV Proton Synchrotron impinging on a 120-mm-long copper target with a diameter of 10 mm. The primary beam is bent downward after the target to a beam dump, and the neutral beam is taken at 0° with respect to the primary beam and is collimated by two brass collimators subtending a solid angle of 154 μsr. Four bending magnets sweep charged secondary particles in the vertical direction. The useful momentum of the K_L^0 ranges from about 2 to 8 GeV/c. A 10-m-long evacuated decay chamber is located at 10.5 m from the target. Two exit windows covered by 50-μm-thick polyester film, which is supported by 60-mg/cm^2 carbon cloth, are located at the downstream end of the decay chamber for charged particles.

Figure 1 shows a plan view of the detector system which is a double-arm spectrometer with particle-identification capability, sandwiching an evacuated beam pipe for transmitting forward produced neutral particles. Each arm of the spectrometer consists of five drift chambers $W1$-$W5$, two bending magnets, two hodoscopes $H1$ and $H2$, a gas Cherenkov counter, an electromagnetic shower counter, and a muon identifier. Helium bags are placed between drift chambers. The total amount of material from the upstream end of the decay chamber up to $W5$ is 8.1×10^{-3} radiation length. $W1$ and $W2$ have the dimensions of 115.2×86.4 cm^2 and $W3$-$W5$ 115.2×115.2 cm^2. Each chamber has four sense-wire planes, X, X', Y, and Y', with a wire spacing of 9 mm. The field wires are placed around each anode wire to form a hexagonal cell structure. The bending magnets are identical and have

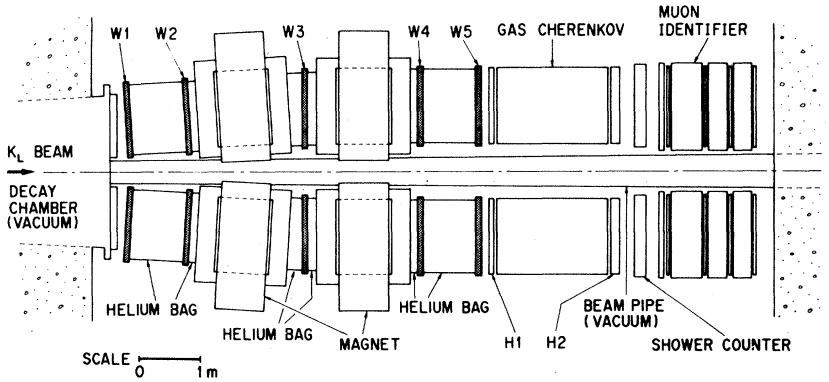

FIG. 1. Plan view of the detector system.

the same magnetic field. The total integrated field strength is 0.79 Tm in each arm corresponding to a transverse-momentum kick of 238 MeV/c. With this value the decay product particles from a nearly transverse $K_L^0 \to \mu e$ decay emerge from the downstream magnet nearly parallel to the K_L^0 direction. The hodoscopes $H1$ and $H2$ placed behind $W5$ are separated by 2 m. Each consists of sixteen vertically arranged scintillators whose dimensions are $7\times115\times1$ cm^3 for $H1$ and $12\times140\times1$ cm^3 for $H2$. The scintillators of $H2$ are staggered so that adjacent counters overlap by 5 cm. Each set of corresponding scintillators in $H1$ and $H2$ covers an angular divergence of 12.5 mrad to accommodate the divergence of the K_L^0 beam.

The gas Cherenkov counter, which is placed between $H1$ and $H2$, is segmented into four cells by mirrors, each of which is viewed by a 5-in. photomultiplier. The radiator is 1.5 m air at atmospheric pressure. It is sensitive to electrons, and the threshold momentum for muons is 4.5 GeV/c. The electromagnetic shower counter consisting of sixteen modules is placed behind $H2$. Each module is made up of ten alternate layers of 6-mm-thick plastic scintillators and 8-mm-thick lead plates. To observe the shower development each module is divided into a four-layer and a six-layer section, which are viewed separately by photomultipliers. The muon identifier consists of four iron blocks with thicknesses of 10, 50, 30, and 30 cm, the 10-cm-thick block being the most upstream end one. The first two blocks are followed by six vertically arranged scintillators and the last two blocks by eight horizontally arranged scintillators. The minimum momenta of muons penetrating the iron blocks are, from the upstream end, 0.4, 1.0, 1.4, and 1.8 GeV/c.

The basic trigger logic for a two-body decay mode is a coincidence between an $H1$ scintillator and the corresponding $H2$ scintillator in both arms of the spectrometer. For the $K_L^0 \to \mu e$ decay signals from the electromagnetic shower counter and the Cherenkov counter in one arm and signals from at least the first two scintillators of the muon identifier in the other arm are also required. The last requirement ensures that the muon momentum is 1.0 GeV/c or greater to reduce the background contamination by pion punchthrough from the predominant $K_L^0 \to \pi e \nu$ decay. The $K_L^0 \to ee$ trigger requires signals from the electromagnetic shower counter and the Cherenkov counter in both arms in addition to the hodoscope requirement, and the $K_L^0 \to \mu\mu$ trigger requires the muon signals as defined above in both arms as well as the hodoscope requirement. The trigger for the $K_L^0 \to \pi^+\pi^-$ decay is made only by the hodoscopes. But since the magnetic fields are tuned for the $K_L^0 \to \mu e$ decay, the π's from the $K_L^0 \to \pi^+\pi^-$ decay do not emerge parallel to the beam, but are bent a little inward. Therefore, the $H1$-$H2$ coincidence requirement mentioned above is relaxed so that either the coincidence between an $H1$ scintillator and the corresponding $H2$ scintillator or the one adjacent to it on the beam pipe side will produce a trigger signal. This trigger rate is suppressed by a factor of 500. No anticoincidence veto is required for the triggers explained above.

Data are taken simultaneously for the four two-body decay modes of the K_L^0 mentioned above with the primary beam intensity of approximately $(1.0\text{–}1.5)\times10^{12}$ protons per pulse. The triggered data include the drift-chamber time-to-digital converter (TDC) information, and TDC and analog-to-digital converter (ADC) information from the scintillation and Cherenkov counters. They are examined by hardware logic to make sure that all five drift chambers have at least one hit per plane (X and/or X' and Y and/or Y'), and by an on-line program that the timing of the charged particles hitting $H1$ is consistent with their being associated with the same decay event (within 5 ns of each other). The data surviving these on-line cuts are recorded on magnetic tape for off-line analysis described below. The dead-time ratio is less than 10%.

A track-finding program selected a track candidate from the drift-chamber hit positions. It was then spatially reconstructed by the spline method. The fitted tracks in both arms were extrapolated in the upstream direction, and the point at which they had the minimum spatial separation was considered as their decay vertex. Only events with the minimum separation less than 1.5 cm were accepted. The vertex point thus obtained also had to lie within the decay chamber and within a cone of less than 9 mrad along the nominal beam direction. Tracks which were spatially very close to magnet pole faces or coils were rejected. In order to eliminate tracks unassociated with K_L^0 decays, the momentum of each track was required to be less than 4.5 GeV/c, and the absolute value of the momentum difference between the two tracks divided by their sum had to be less than 0.5 to eliminate events with obvious momentum imbalance. Furthermore, the momenta of a track in the upstream and downstream halves of the spectrometer were checked for consistency to reject any particle which had decayed in flight during the passage through the spectrometer.

Using the information on particle identification, the momenta and coordinates of the two tracks, their effective mass and its momentum as well as the direction of the line connecting the target and the decay vertex were calculated. If the tracks are due to a two-body decay of the K_L^0, the effective mass should be close to the K_L^0 mass, and the angle θ between the target-to-vertex direction and the vector sum of the two track momenta should be close to zero. Figure 2(a) shows a scatter plot of the effective mass (m) vs θ^2 for $\pi\pi$ events, and Fig. 2(b) is the mass distribution. It is centered at the K_L^0 mass with a standard deviation of 1.3 MeV/c^2, which represents the mass resolution of the detector system and the spatial reconstruction program. Figure 2(c) is the distribution of θ^2 for the $\pi\pi$ events. Since these distributions are known to be nearly the same for the μe, ee, and $\mu\mu$ events from a Monte Carlo calculation which did not include radiative decay modes such as $\pi^+\pi^-\gamma$, $ee\gamma$, and $\mu\mu\gamma$, we have adopted the following fiducial region for acceptable K_L^0 two-body decay events: $493\ \text{MeV}/c^2 < m < 502\ \text{MeV}/c^2$ and $\theta^2 < 3(\text{mrad})^2$, which is about three times their resolutions.

Figures 3(a), 3(b), and 3(c) show the scatter plots of the effective mass versus θ^2 for the μe, ee, and $\mu\mu$ events with the above fiducial region superposed. No event is seen in the fiducial region in the μe and ee plots, and 54 events are found in the $\mu\mu$ plot. The number of $\pi\pi$ events in the fiducial region is 4.2×10^4, corresponding to a sensi-

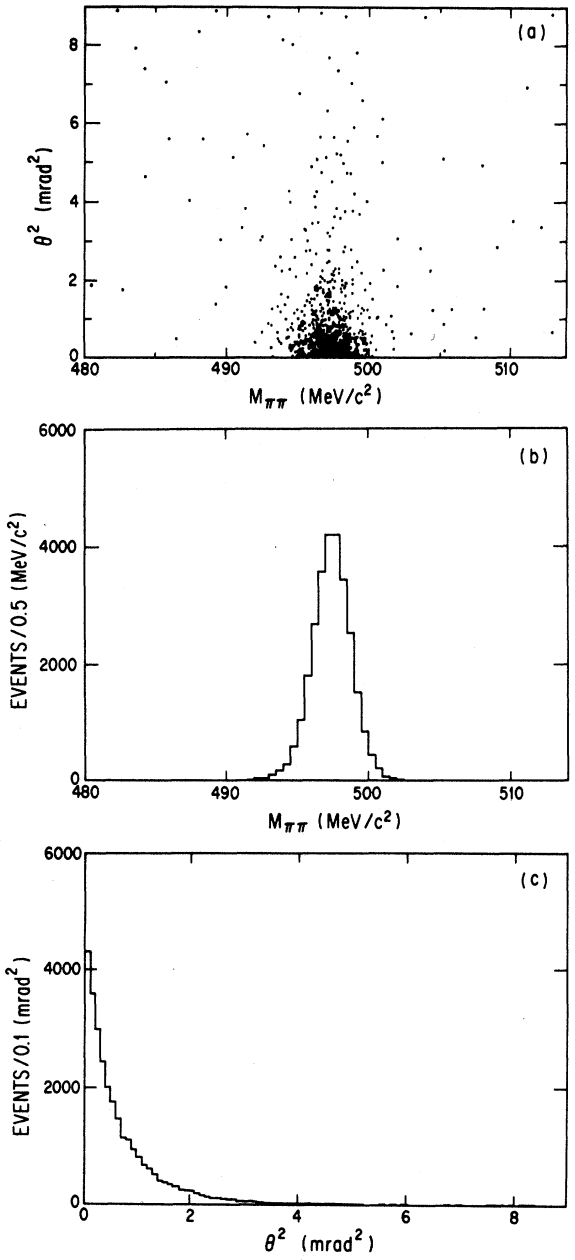

FIG. 2. (a) $\pi\pi$ effective mass vs θ^2 based on a representative sample of 1000 events; (b) $\pi\pi$ effective-mass distribution for events with $\theta^2 < 3$ mrad^2; and (c) θ^2 distribution for events with $\pi\pi$ effective mass in the range 493–502 MeV/c^2.

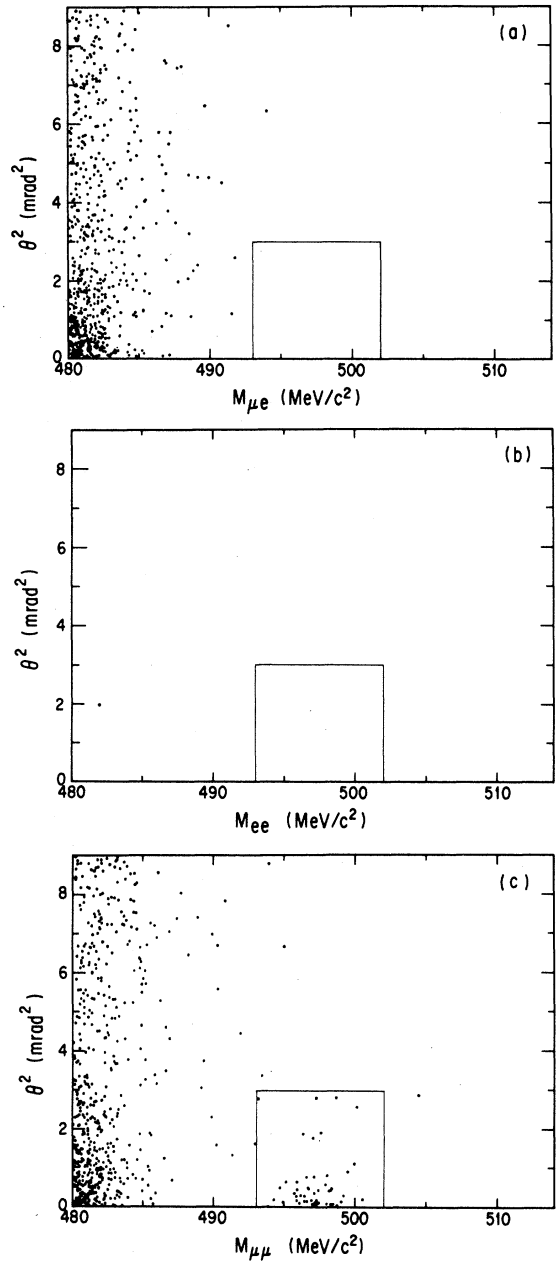

FIG. 3. (a) μe effective mass vs θ^2; (b) ee effective mass vs θ^2; and (c) $\mu\mu$ effective mass vs θ^2. The rectangle in each figure represents the fiducial region.

tivity of 1.1×10^{-10} after correcting for the trigger suppression factor and the $K_L^0\to\pi^+\pi^-$ branching ratio of 2.04×10^{-3}.[6] For the leptonic decay modes the acceptance ratio with respect to the $\pi\pi$ mode (0.98 for μe, 0.96 for ee, and 0.90 for $\mu\mu$) and the particle identification efficiency (0.61 for μe, 0.47 for ee, and 0.79 for $\mu\mu$) are taken into account. From the 54 $\mu\mu$ events we get an absolute branching ratio of $(8.4\pm1.1)\times10^{-9}$. The error is statistical only. This value is consistent with the current value of $9.5^{+2.4}_{-1.5}\times10^{-9}$.[6] The upper limits of the $K_L^0\to\mu e$ and $K_L^0\to ee$ branching ratios are calculated to be $B(K_L^0\to\mu e)<4.3\times10^{-10}$ and $B(K_L^0\to ee)<5.6\times10^{-10}$, respectively, at 90% confidence level.

We are grateful to the operating crew of the KEK PS and the members of the Beam-Line Group, the Electronics and Online Groups, and the Machine Shop for their indispensable help. We express our sincere gratitude to Professor T. Nishikawa, Professor H. Sugawara, Professor N. Nakai, and members of the Administrative Office and the Physics Department of KEK for their encouragement and support.

*Present address: IBM Research, Tokyo Research Laboratory, Sanbancho, Chiyoda-ku, Tokyo 102, Japan.
†Present address: NEC Corp., Microelectronics Research Laboratory, Sagamihara, Kanagawa 229, Japan.

[1]R. D. Cousins *et al.*, Phys. Rev. D **38**, 2914 (1988).
[2]S. F. Schaffner *et al.*, Phys. Rev. D **39**, 990 (1989).
[3]G. L. Kane and R. E. Shrock, in *Intense Medium Energy Sources of Strangeness,* proceedings of the Santa Cruz, California, Workshop, 1983, edited by T. Goldman, H. E. Haber, and H. F.-W. Sadrozinski (AIP Conf. Proc. No. 102) (AIP, New York, 1983), p. 123.
[4]E. Jastrzembski *et al.*, Phys. Rev. Lett. **61**, 2300 (1988).
[5]A. Barroso, G. C. Branco, and M. C. Bento, Phys. Lett. **134B**, 123 (1984); E. Eichten, I. Hinchliffe, K. D. Lane, and C. Quigg, Phys. Rev. D **34**, 1547 (1986); B. A. Campbell, *ibid.* **28**, 209 (1983); J. C. Pati and H. Stremnitzer, Phys. Lett. B **172**, 441 (1986); I. I. Bigi, G. Köpp, and P. M. Zerwas, Phys. Lett. **166B**, 238 (1986); W. Hou and A. Soni, Phys. Rev. Lett. **54**, 2083 (1985); O. Shanker, Nucl. Phys. **B206**, 253 (1982); L. J. Hall and L. J. Randall, *ibid.* **B274**, 157 (1986); B. A. Campbell, J. Ellis, K. Enqvist, M. K. Gaillard, and D. V. Nanopoulos, Int. J. Mod. Phys. A **2**, 831 (1987); N. G. Deshpande and R. J. Johnson, Phys. Rev. D **27**, 1193 (1983).
[6]Particle Data Group, G. P. Yost *et al.*, Phys. Lett. B **204**, 17 (1988).